Synthesis of microstructure diamond and related materials at different CH_4/H_2 in the reactant gases

Scientific research paper

Somayeh Asgary

[1]*Department of Physics, West Tehran Branch, Islamic Azad University, Tehran, Iran*

ARTICLE INFO

Article history:
Received 28 February 2024
Revised 9 May 2024
Accepted 17 June 2024
Available online 20 December 2024

Keywords
Diamond structure
PECVD method
Raman
XRD

ABSTRACT

Diamond structure were deposited on gold coated Si substrate successfully using DC-PECVD technique at different CH_4/H_2 in the reactant gases (CH_4/H_2 = 2, 5 and 7 vol. %). Characterization of diamond structure has been investigated in detail by X-ray diffraction (XRD), Raman spectroscopy (RS), atomic force microscopy (AFM) and scanning electron microscopy (SEM). The results determine the effect of the different CH_4/H_2 in the reactant gases on the crystallinity, phase, surface morphology and microstructure. The XRD patterns show polycrystalline structure with diamond (111) preferred growth orientation and better crystalline quality at middle methane concentrations. The first order Raman peak for diamond phase was more intense at middle methane concentrations, while a relatively broad G-band from the graphitic types was appearance. Diamond structures with large grain sizes in the micron or tens of micron range have homogenous surfaces.

1 Introduction

Chemical bonds of the valence electron of carbon forms in three different hybridizations: sp, sp^2,and sp^3 which lead to formation of various carbon nanostructures [1].

Graphite and diamond are famous allotropes, though the carbon phase diagram is of great interest to chemists and physicists such as nanotubes [2], fullerenes [3], amorphous carbon [4], and graphene [5].

Diamond consists of 100% sp^3 carbon bond hybridization. The sp^3 carbon bond hybridization formed a perfect symmetry of the diamond structure, which affords brilliant properties like excellent thermal conductivity, very high hardness, high electrical resistivity, optical transparency, wide band gap, chemical inertness, and low wear rate in various tribological systems [6-7].

Graphite consists of sp^2 carbon bond hybridization and has anisotropic properties in one direction; though in the vertical direction only a weak Van der Waals force is acted. The sp^2 hybridization consequences low electrical resistivity, low hardness, low friction, and high wear rate [8-9].

In amorphous carbon, atoms joined together with a disordered network with a combination of sp^3, sp^2 coordinated bonds and sp^1 sites. Diamond-like carbon (DLC) is the famous family of amorphous carbon that consists of a high fraction of sp^3 bonds [10].

Based on the fraction and percentage of sp^2 and sp^3 bonds and the hydrogen content, there are four different forms of DLC layers: tetrahedral amorphous carbon (ta-C), amorphous carbon (a-c), hydrogenated tetrahedral

*Corresponding author.
Email address: Sima198124@Yahoo.com
DOI: 10.22051/jitl.2024.46388.1107

amorphous carbon (ta-C:H), and hydrogenated amorphous carbon (a-C:H, some containing up to about 50 at.% hydrogen) [11-13]. The a-C layers can have 85% or more sp^3 bonds whereas the a-C:H layers naturally have sp^3 fractions smaller than 50% [14].

There are numerous chemical and physical methods for synthesizing diamond. Production of diamond (especially single crystal) with a few nm and several mm particles sizes typically need high pressures and high temperatures in order to convert graphite into diamond [15].

Diamond is an important material in science because of its superior properties and notable applications in technology such as optoelectronic devices on quantum computers [16], Raman laser optical lens [17], X-ray optical assembly [18], high-power optical lens used as a megawatt cyclotron in a nuclear fusion reactor [19], high power density radiator [20], a biochip substrates and sensors [21], bipolar diamond electronics [22], and components of diamond material used for scientific research under high pressure conditions [23].

Deposition of diamond structure in the form of thin layers has opened different new applications for diamond, like sensors, optical windows, heat spreaders, and cutting tools [24].

Diamond layers are deposited in several techniques like laser ablation [25-26] and plasma discharge [27-28] Nevertheless chemical vapor deposition (CVD) is the well-known way for deposition of diamond thin films. Numerous CVD based techniques are also used like hot filament techniques [29], plasma enhanced CVD (PECVD) [30-31], and employment of a combustion-flame [32].

Growth of diamond layers by the CVD method must be accompanied under non-equilibrium conditions. Under normal conditions, graphite structure is a more stable than diamond structure.

Methane is generally used as the carbon source for CVD diamond growth. Furthermore, during the CVD process, hydrogen radicals (atomic hydrogen) play different roles such as termination of carbon dangling bonds, abstraction reactions, and eliminating the non-diamond materials containing graphite that is formed on the diamond surface [33-34].

One of the key procedures in the growth of diamond films on foreign substrates such as silicon is nucleation [35]. Carbon and silicon are belonging to group IV members, but silicon has the larger atomic number. Diamond and silicon have the same crystalline structure, so it is expected that diamond can act as the basic material for the next generation of optoelectronic, high-power electronic, bio/chemical electronic, etc. Diamond displays electrical properties similar to silicon, with exciting physical properties [36].

The PECVD technique has become an important technology for deposition of diamond or DLC films in contrast to other methods owing to its high deposition rate, low deposition temperature, low particulate levels, purity, good control over stoichiometry, and possibility of deposition on a large area [37]. Control over the film thickness, impurity, defect levels, and morphology is possible with this process. PECVD allows the economical production to deposit diamond thin films. Neither the reactant gases (CH_4 and H_2) nor the process are fundamentally expensive [38].

Different parameters in chemical growth process such as reacting gases; bias voltage etc. can be used for deposition of diamond films [39-41]. Mucha et al. [42] reported deposition of polycrystalline diamond films using the PECVD technique as a function of CH_4 [0.2-4%] and O_2 [0-3%] concentrations. The prepared films have been characterized by measurements of morphology, surface roughness, deposition rate, stress and impurity levels (C-H and amorphous-graphitic carbon). Pinneo et al. [43] investigated the feasibility of PECVD diamond films as a potential electronic material. Jiao et al. [44] reported the synthesis of ultra-nano crystalline diamond films, grown using microwave plasma-enhanced chemical vapor deposition with gas mixtures of Ar– 1% CH_4 or Ar– 1% CH_4 – 5% H_2.

In this study, we investigated the effect of methane concentrations (CH_4/H_2 2, 5, 7 vol. %) on the growth of diamond coatings on gold coated Si substrates by the DC plasma-enhanced chemical vapor deposition (DC-PECVD) system. Concentration of CH_4 most toughly affected the amount of diamond bonding relative to the amount of graphitic bonding. Actually, the gas mixture ratio on deposition of diamond films has a great influence on the surface morphology and physical properties of the diamond films.

Zhu and et al. [45] reported results of structural development of diamond layers with different ratios of gas mixture. Kobashi et al. [46] synthesized the polycrystalline diamond films with (111) growth orientation at low CH_4 concentrations that changes to (100) growth orientation when the CH_4 concentration is increased, with a very narrow concentration range of 0.4% causing this transformation. The effect of variation in CH_4/Ar gas ratio on the structure, transmission, refractive index, and hardness of the DLC layers were studied by Samadi et al. [47]. The results showed that the CH_4/Ar gas ratio strongly affected the chemical composition and consequently the mechanical and optical properties of the DLC films.

Because of the C-H and C-H-O systems, numerous parts of the gas phase chemistry and several surface procedures have not been opened. The results provide a more comprehensive understanding of the methane concentrations influence on diamond structural and morphological features and could help in controlling the topographical parameters according to the surface morphology requirements suitable for photovoltaic applications [48].

2 Experimental details

In this work, diamond layers are deposited on gold coated Si substrates by using a DC-PECVD technique. Thin gold layer acts as the catalysts. The substrates were p-type silicon (100) wafers that were ultrasonically pre-cleaned with acetone, ethanol, and de ionized water for 15 minutes. Then the Si substrates coated with a thin layer of gold promote the nucleation of crystalline diamond on the surface.

The proses of the diamond growth were done in two steps: deposition and post annealing. The deposition system is consisting of a vacuum unit equipped with both rotary and turbo molecular pumps and a DC plasma generator. There is a cylindrical Pyrex chamber with a diameter of 28 cm at the central part of the DC-PECVD. All cleaned substrates were placed to the central part of the DC-PECVD system. The base pressure on the growth system was reserved at 1×10^{-2} Torr, after the chamber was pre-evacuated using a rotary pump. A mixture of CH_4/H_2 (CH_4/H_2 2, 5, 7 vol. %) with flux rates of 130 sccm was fed into the reaction chamber for deposition of diamond structures. The chamber pressure was adjusted at 20 Torr. The applied current and voltage in this experiment were 40 mA and 600 V respectively.

The temperature of the substrates was monitored by a thermocouple that kept 300°C. The deposit time was 50 minutes.

During growth process by the PECVD method, the surface of diamond is bombarded by hydrogen radicals. Hydrogen acts as the etching gas to improve the diamond nucleation, by reducing the graphite content on the surface of diamond films [49]. Diamond is also etched by reactions with hydrogen radicals, but the etching rate of diamond is lower than non-diamond structure of carbon.

Presence of a high concentration of atomic hydrogen and CH_4 radicals is an essential condition for a successful deposition of microcrystalline diamond [50-51].

With a different combination of hydrogen and methane gases which depends on many factors such as the substrate temperature, composition, system pressure, and the flow rate of the incoming gas, various species are formed. The deposition conditions are summarized in Table 1 while the deposition schematic is shown in Fig.1.

Table 1. Growth conditions of diamond structure on gold coated Si substrate.

Sample	Combination of CH_4/H_2 (% vol)	Deposition time (min)
S_1	2	50
S_2	5	50
S_3	7	50

The evolution of microstructure and topography of the coatings at different CH_4 /H_2 gas mixture was systematically analyzed by X-ray diffraction (XRD) that a Cu-k-alpha radiation (1.54°A) was used, operated at 40 Kv and 30 mA, with 2Θ ranging from 20°-90° and atomic force microscopy (AFM) analysis (Park Scientific instruments, Auto probe CP) in contact mode. The samples were characterized by scanning electron microscope (S-3400, Hitachi, Japan). Raman analysis is a useful technique to understand carbonaceous materials. Details of Raman analyses were carried out by using excitation laser of 514 nm to recognize the chemical bonding nature of the diamond coatings.

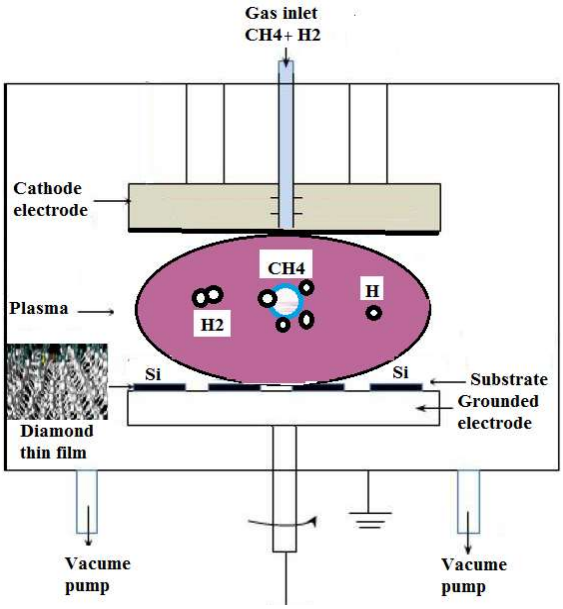

Figure 1. Schematic of deposition proses: PECVD system.

3. Results and discussion

3.1 XRD

The X-ray diffraction (XRD) technique is used to confirm diamond synthesis, identify the crystalline structure, impact of annealing temperature on crystal quality, amounts of d-spacing and grain size and data about preferential orientation, residual strain and dislocation density.

Figure 2 shows the XRD spectra of diamond structure deposited on gold coated Si substrates at different CH_4 /H_2 in the reactant gases.

At sample 1, the dominant peaks were identified at 2θ = 44.27° corresponding to the (111) plane of the cubic diamond (JCPDS card No.01-075-0410). Two peaks at 24.8° and 77.7° were artifacts from the (0015) and (113) graphite planes, respectively (JCPDS card No.01-074-2329). The diffraction peak at ~ 69.5° corresponded to (100) plane of silicon substrate. The diffraction peaks at 2θ = 37.9° and 64.5° are related to (111), and (220) plans of gold nanoparticles (JCPDS card No.00-004-0784).

At sample 2, the XRD spectrum shows a well-defined peak at 43.9° and a weak peak at 81.8° assigned to nano diamond (111) [52] and diamond (1031) orientations, respectively. A low-intensity peak at 2θ = 32.9° is related to the Buckminster fullerene (511) plane (JCPDS card No.00-044-0558). At this sample, the (111) crystalline plane was slightly more intense.

The peak with higher intensity indicates more diamond material diffracted by the X-ray beam. However, different factors effect on the peak intensity, such as the surface topography of the prepared sample and other instrumental factors like alignment and beam intensity.

The higher-intensity diamond peak in all samples was located at 2θ = 43.9°, which belongs to the reflection of crystal plane with Miller indices of (111), showing the preferential orientation along (111) plane (JCPDS card No. 00-002-1248). Increasing the sharpness and resolution of the peaks, indicates improvement of the crystallinity of the sample, while the sample contains substantial graphitic impurities.

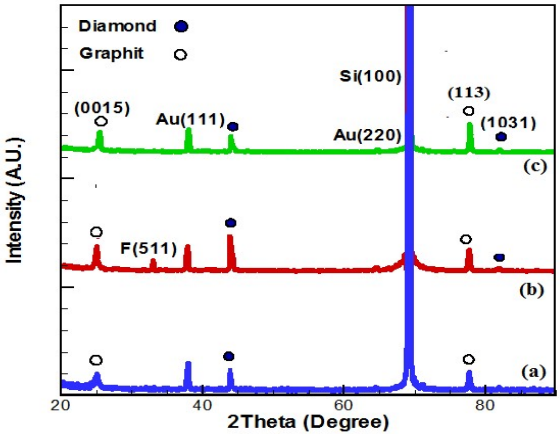

Figure 2. XRD diffraction pattern of deposited diamond structure at different combination of CH_4 /H_2: (a) sample 1: 2%, (b) sample 2: 5%, (c) sample 3: 7%.

Thermodynamics determines the preferred orientations according to the minimization of total energy (sum of surface and strain energies). Since the (111) is the greatest close-packed plane with the lowest surface energy, it seems that the strain energy was dominant. It is determined that the crystallinity of the sample is affected not only by the initial growth parameters, but also by the evolution of the conditions during deposition process.

By increasing the combination of CH_4 /H_2 to 7% vol, the Buckminsterfullerene peaks completely disappear. This sample showed a higher content of a non-diamond

phase. Maybe in the CH_4/H_2 7% vol, diamond would be etched faster than that CH_4/H_2 5% vol [53].

3. 2 Raman Spectroscopy

X-ray diffraction is sensitive to the existence of crystalline carbons like graphite and diamond while, it is less sensitive to presence of amorphous carbon. In comparison, Raman scattering is around 50 times more sensitive to p-bonded amorphous carbon structure and graphite than the phonon band of diamond, so it is often used to characterize CVD diamond structures.

Raman analysis provides distinguishable signatures of different arrangements of carbon (sp^2 and sp^3).

The difference between graphite and diamond bonding can describe as carbon network solids joined by covalent bonding. In diamond, the carbon atoms are covalently bonded using sp^3 hybrid. The carbon atoms in graphite layers are covalently bonded by hexagons structure and the layers bonded with weak Van der Waals bonds [54].

Figure 3 indicates the Raman spectrum of deposited graphite/diamond structure on gold coated Si substrate at different combination of CH_4/H_2 in the reactant gases.

Raman spectrum of sample 1 showed a first-order diamond (sp^3 carbon) peak at 1335 cm^{-1} that is related to the vibrations of the two interpenetrating cubic sublattices [55]. This result has been confirmed by other scientists [56-57].

It is noted that the diamond peak is shifted to a larger wave number than natural diamond peak (1332 cm^{-1}), demonstrating presence of the residual compressive stress in the sample [58].

Based on the Raman analysis, in sample 2, the first-order Raman peak related to diamond was more intense (confirmed by X-ray diffraction result).

Low intensity Raman scattering in the broad range ~ 1450– 1490 cm^{-1} is related to the graphite band caused by the sp^2 bonded carbon.

Moreover, there is also a broad peak located at ~ 1572–1592 cm^{-1}. This band is known as the G-band related to the non-diamond, graphitic carbon phase [59]. The G peak for carbon materials invented from vibrations of any pair of sp^2 sites in chain or ring arrangements [60].

The peak at ~ 1490 cm^{-1} is related to C=C stretching vibration modes of trans-poly acetylene (TPA) hydrocarbon chains on inter crystallite boundaries.

We can see that the G-peak is shifted to higher wave numbers. There are two main reasons for moving the G-peak positions to higher wave numbers in the Raman spectra of carbon-based materials. The first one is the high sp^2 content or cluster size and the second one is high compressive stress [61].

According to Ralchenko et al., when diamond transforms, graphite increases in the grain boundaries that causes compressive stress [62].

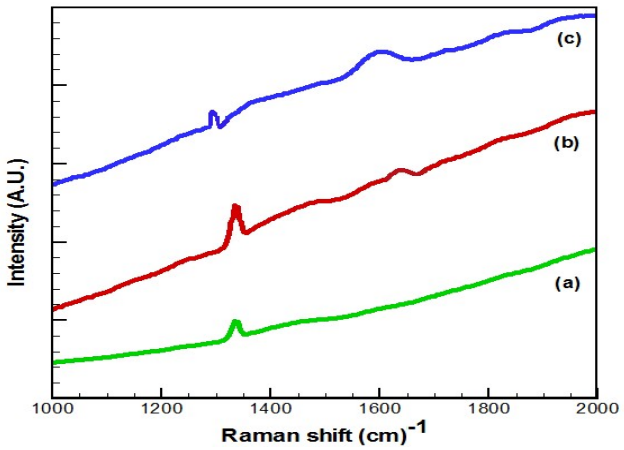

Figure 3. Raman spectrum of deposited diamond structure at different combination of CH_4/H_2: (a) sample 1: 2%., (b) sample 2: 5%, (c) sample 3: 7%.

The diamond Raman signal peak was more intense in CH_4/H_2 5% vol and a higher amount of graphite crystals at higher CH_4 concentration in the reactant gases

3. 3 AFM

AFM offers a three-dimensional image of a solid surface to study morphology of the films and roughness by scanning the surface through a mechanical tip.

The 2D, 3D and histogram topography of the surfaces is shown in Fig. 4.

At sample 1, the AFM image showed a very flat and smooth surface morphology with relative uniform spherical particles and grain size of 30-32 nm.

The AFM image of sample 2 showed the the homogeneity structure of the film was reduced and contains separate grains with average sizes around 35 nm. The root mean square surface roughness of the films resulting from AFM data is 16.63 nm.

At sample 3, the surface is composed of separate particles with a typical size between 50-55 nm and surface roughness of 27.57 nm.

It seems that increasing the CH_4 concentration in the reactant gases, leads to increasing the RMS roughness values and surface covered by relatively large grains (Fig.5).

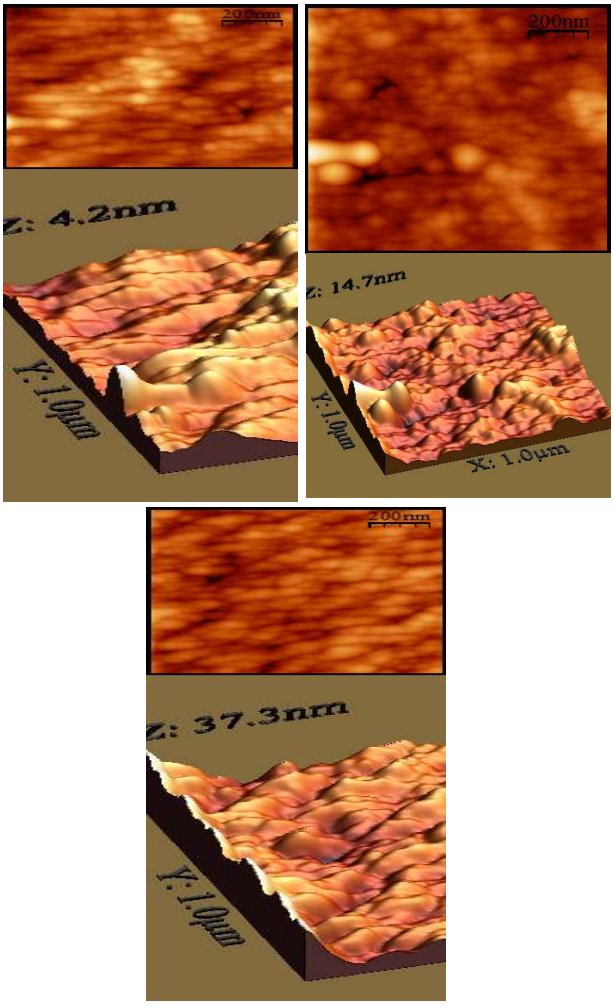

Figure 4. 3D and 2D AFM images of the diamond structures on gold coated Si substrate at different combination of CH_4/H_2: (a) sample 1: 2%., (b) sample 2: 5%, (c) sample 3: 7%.

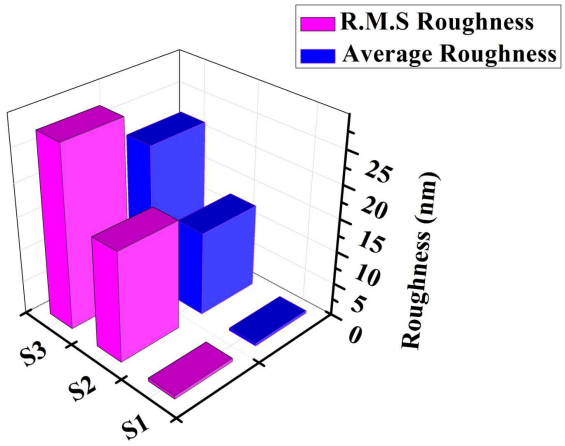

Figure 5. RMS roughness and average roughness of samples.

Presence of large islands on the surface of thin films may be due to agglomeration of diamond/graphite crystallites [63].

3. 4 FE-SEM

The FE-SEM analysis was prepared to study the surface morphology. The analysis was carried out at different scales. The plan view FE-SEM micrographs in Fig. 6 displays morphologies of the diamond structure which were grown at different CH_4/H_2 in the reactant gases.

Sample 1 consists of large diamond crystallites with rectangular, triangular, and cubic structures. The crystallites size of approximately 10 micron.

Highly crystalline diamond crystals were observed in sample 2. It was clearly visible that the size distribution of diamond micro particles was uniform and most of them have cubic and rectangular shapes. The particle size of grown diamond crystals was 12-15 micron that would contain some non-diamond phase.

Sample 3 consists of micro scale grains with well-defined shape that grows from smaller crystallites. The image mostly included particles with the hexagonal structure. As can be seen, in some places, sample 3 is more condense in comparison with the other samples. The average size of these crystals is 15-18 micron and distinguishable grain boundaries are observed in some places. It seems that during the deposition process, small diamond/graphite particles form on the surface of bigger grains, resulting in the occurrence of re-nucleation at higher methane concentration.

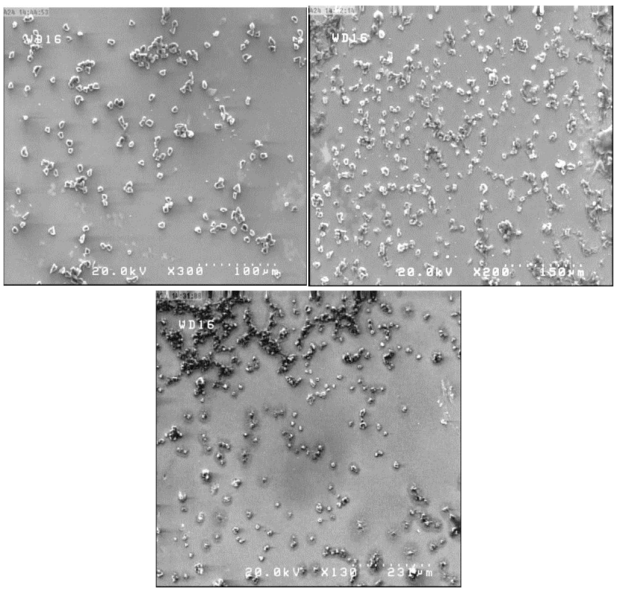

Figure 6. FE-SEM images of samples at different combination of CH_4/H_2: (a) sample 1: 2%., (b) sample 2: 5%, (c) sample 3: 7%.

From the Raman spectra in Fig.3, the graphite peak was clearly evident in sample 3 and the film had a relatively higher non-diamond (graphitic) component. This seems to be the main reason for appearance of dark regions in the middle of this sample.

4 Conclusions

Diamond thin films with microcrystals size grains were deposited on gold coated Si substrates by the DC-PECVD method. For growth of diamond structures, a mixture of CH_4/H_2 with a different ratio of CH_4 and H_2 mixture gas (CH_4/H_2 = 2, 5 and 5 vol. %) was fed into the reaction chamber during the deposition process. The results showed that the mechanism of diamond growth depends strongly on the ratio of CH_4 and H_2 mixture in the reactant gases. The x-ray diffraction patterns show clear diffraction peaks that are associated with the growth of diamond microcrystals with orientation in (111) plane and low-intensity peaks related to the graphite crystals. Well-facetted microcrystalline diamond structure with micron grain sizes with regular distribution is observed. The first-order Raman peak from diamond phase was much more apparent and relatively broad G band from the graphitic species was observable in the middle methane concentration. The grain size increases and therefore surface roughness increases with increasing methane concentration.

References

[1] T. Lühmann, et al., "Investigation of the graphitization process of ion-beam irradiated diamond using ellipsometry, Raman spectroscopy and electrical transport measurements." Carbon N Y. **121** (2017) 512

[2] J. Prasek, et al., "Methods for carbon nanotubes synthesis - Review." Journal of Materials Chemistry, **21** (2011) 15872.

[3] M. Prato, "[60] Fullerene chemistry for materials science applications." Journal of Materials Chemistry, **7** (1997) 1097.

[4] J. Robertson, "Diamond-Like Amorphous Carbon. Materials Science and Engineering: R: Reports." **37** (2002) 129.

[5] C.N.R. Rao et al., "Graphene: the new two-dimensional nanomaterial." Angewandte Chemie International Edition**, 48** (2009) 7752.

[6] C. Artini et al., "Diamond–metal interfaces in cutting tools: a review." Journal of Materials Science, **47** (2012) 3252.

[7] J. E. Field (Ed.), Properties of Natural and Synthetic Diamond, Academic Press, London, 1999.

[8] R. Sengupta et al., "A Review on the Mechanical and Electrical Properties of Graphite and Modified Graphite Reinforced Polymer Composites." Progress in Polymer Science, **36** (2011) 638.

[9] H. O. Pierson, Handbook of Carbon, Graphite, Diamonds and Fullerenes: Processing, Properties and Applications, Noyes Publications, New Jersey, 1993.

[10] J. Vetter, "60 years of DLC coatings: historical highlights and technical review of cathodic arc processes to synthesize various DLC types, and their evolution for industrial applications." Surface and Coatings Technology, **257** (2014) 213.

[11] D. R. McKenzie, "Tetrahedral bonding in amorphous carbon." Reports on Progress in Physics, **59** (1996) 1611.

[12] P. Koidl et al., "Plasma Deposition, Properties and Structure of Amorphous Hydrogenated Carbon Films." Materials Science Forum, **52** (1991) 41.

[13] G. M. Pharr et al., "Hardness, elastic modulus, and structure of very hard carbon films produced by cathodic-arc deposition with substrate pulse biasing." Applied physics letters, **68** (1996) 779.

[14] A. Grill, "Diamond-like carbon: state of the art." Diamond and Related Materials **8** (1999) 428.

[15] A.Kh. Khachatryan et al.," Graphite-to-diamond transformation induced by ultrasound cavitation." Diamond & Related Materials **17** (2008) 931.

[16] D. D. Awschalom et al., "The Diamond Age of Spintronics." Scientific American, **297** (2007) 84.

[17] R. P. Mildren et al., CVD-diamond external cavity Raman laser at 573 nm." Optics Express, **16** (2008) 18950.

[18] L. E. Berman et al., "Diamond crystal X-ray optics for high-power-density synchrotron radiation beams." Nuclear Instruments & Methods in Physics Research **329** (1993) 555.

[19] M. Thumm, "Progress on gyrotrons for ITER and future thermonuclear fusion reactor." IEEE Transactions on Plasma Science, **39** (2011) 971.

[20] A. J. Maclean et al., "Limits on efficiency and power scaling in semiconductor disk lasers with diamond heatspreaders." R. B. Birch, P.W Roth and et al. Journal of the Optical Society of America B, **26** (2009) 2228.

[21] C. E. Nebel et al., "Diamond and biology." Wiley-VCH Verlag GmbH & Co. KGaA, **93** (2008) 439.

[22] S. Koizumi et al., 'Ultraviolet emission from a diamond pn junction." Science, **292** (2001) 1899.

[23] R. J. Hemley et al., "Growing Diamond Crystals by Chemical Vapor Deposition." 1(2005) 105.

[24] R. S. Balmer et al., "Chemical vapour deposition synthetic diamond: Materials, technology and applications." Journal of Physics Condensed Matter, **21** (2009) 364221.

[25] A. Grill, "Amorphous carbon based materials as the interconnect dielectric in ULSI chips."Diamond and Related Materials **10** (2001) 234.

[26] Y. Komatsu et al., "Application of *diamond*-like carbon films to the integrated circuit fabrication process." Diamond and Related Materials, **8** (1999) 2018.

[27] J. H. Sui et al., "Effect of diamond-like carbon (DLC) on the properties of the NiTi alloys." Diamond and Related Materials. **15** (2006) 1720.

[28] O.L. Eryilmaz et al., 'Deposition, characterization, and tribological applications of near-frictionless carbon films on glass and ceramic substrates." Journal of Physics and Condense Matter, **18** (2006) 1751.

[29] J. Robertson, "Diamond-Like Amorphous Carbon." Materials Science Engineering, **37** (2002) 129.

[30] Y. Liou et al., "Effect of oxygen in diamond deposition at low substrate temperatures." Applied Physics Letters, **56** (1990) 437.

[31] F. Qian et al., "High intensity femtosecond laser deposition of diamond-like carbon thin films." Journal of Applied Physics, **86** (1999) 2281.

[32] S. Logothetidis, "Hydrogen-free amorphous carbon films approaching diamond prepared by magnetron sputtering." Applied Physics Letters, **69** (1996) 158.

[33] Y. Yamazaki et al., "Structural change in diamond by hydrogen plasma treatment at room temperature." Diamond and Related Materials, **14** (2005) 1939.

[34] T. Lühmann et al., "Investigation of the graphitization process of ion-beam irradiated diamond using ellipsometry, Raman spectroscopy and electrical transport measurements." Carbon, **121** (2017) 512.

[35] P. Bergonzo et al., "3D shaped mechanically flexible diamond microelectrode arrays for eye implant applications: the MEDINAS project." IRBM News, **32** (2011) 91.

[36] N. Tokudan," Homoepitaxial Diamond Growth by Plasma-Enhanced Chemical Vapor Deposition." Novel Aspects of Diamond, **1** (2014) 1211.

[37] D. Tither et al., "Application of diamond-like carbon coatings deposited by plasma-assisted chemical vapour deposition onto metal matrix composites for two-stroke engine components." Material Science, **32** (1995) 1931.

[38] S. M. Ojha., "Plasma-Enhanced Chemical Vapor Deposition of Thin Films." Physics of Thin Films, **12** (1982) 237.

[39] A. Erdemir et al., 'Friction and wear performance of diamond-like carbon films grown in various source gas plasmas.' Surface and Coatings Technology, **120-121** (1999) 589.

[40] H. Liu et al., "The tribological characteristics of diamond-like carbon films at elevated temperatures." Thin Solid Films, **346** (1999) 162.

[41] H. Yamada et al., "Field Electron-Emission from a-CNx:H Films Formed on Al Films Using Supermagnetron Plasma CVD." Thin Solid Films, **270** (1995) 220.

[42] J. A. Mucha et al., "Growth and Characterization of PECVD Diamond Films." Materials Research Society symposium proceedings, **250** (1982) 357.

[43] M. G. Peters et al., "PECVD (Plasma Enhanced Chemical Vapor Deposition) diamond thin films for research instrumentation." Crystallume Proprietary Information, (1988) 1.

[44] S. Jiao et al., "Microstructure of ultrananocrystalline diamond films grown by microwave Ar-CH_4 plasma chemical vapor deposition with or without added H_2." A. Sumant, M. A. Kirk, D. M. Gruen, A. R. Krauss et al., Journal of Applied Physics, **90** (2001) 118.

[45] W. Zhu et al., "Crystal growth and gas ratio effect of diamond films synthesized by oxyacetylene flames." Diamond and Related Materials, **2** (1993) 491.

[46] K. Kobashi et al., "Synthesis of diamonds by use of microwave plasma chemical-vapor deposition: Morphology and growth of diamond films." Physica; Review B, **38** (1988) 4067.

[47] M. Samadi et al., "The influence of gas flow rate on the structural, mechanical, optical and wettability of diamond-like carbon thin films." Optical and Quantum Electronics, **50** (2018) 1.

[48] A. Varade et al., "Diamond-like carbon coating made by RF plasma enhanced chemical vapour deposition for protective antireflective coatings on germanium." Procedia Engineering, **97** (2014) 1452.

[49] K. C. Yang et al., "Influence of intermittently eatching on quality of CVD diamond thin films." Transactions of Nonferrous Metals Society of China, **16** (2006) 321.

[50] Y. A. Mankelevich et al., "Three-dimensional simulation of a HFCVD reactor." Diamond and Related Materials, **17** (2008) 1021.

[51] M. Frenklach, "The role of hydrogen in vapor deposition of diamond." Applied Physics, **65** (1989) 5142.

[52] B.H. Al-Tamimi et al., "Synthesis and characterization of nanocrystalline diamond from graphite flakes via a cavitation-promoted process." Heliyon **5,** (2019) 01682.

[53] Byeong-Kwan Song et al., "Unusual Dependence of the Diamond Growth Rate on the Methane Concentration in the Hot Filament Chemical Vapor Deposition Process." Materials. **14** (2021) 426.

[54] C. Lee et al., "Anomalous Lattice Vibrations of Single- and Few-Layer MoS2." ACS Nano, **4** (2010) 2695.

[55] A. Rakha et al., "Ion Irradiation-Induced Modifications of Diamond Nanorods Synthesised by Microwave Plasma Chemical Vapour Deposition." Journal of Experimental Nanoscience, **8** (2013) 555.

[56] B.V. Spitsyn et al., "Vapor growth of diamond on diamond and other surfaces." Journal of Crystal Growth **52** (1981) 219.

[57] S.A. Solin et al., "Raman Spectrum of Diamond ." Physical Review B, **1** (1970) 1687.

[58] K. Huang et al., "The oxidization behavior and mechanical properties of ultrananocrystalline diamond films at high temperature annealing." Applied Surface Science, **317** (2014) 11.

[59] W. Zhang et al., Anodic Electrochemical Pretreatment Time and Potential Affect the Electrochemical Characteristics of Moderately Boron-Doped Diamond Electrode." Collection of Czechoslovak Chemical Communications, **73** (2008) 73.

[60] X.J. Hu et al., "n-type conductivity and phase transition in ultrananocrystalline diamond films by oxygen ion implantation and annealing." Journal of Applied Physics, **109** (2011) 053524.

[61] J.K. Shin et al., "Effect of residual stress on the Raman-spectrum analysis of tetrahedral amorphous carbon films." Applied Physics Letters, **78** (2011) 631.

[62] V. Ralchenko et al., 'Structure and properties of high-temperature annealed CVD diamond." Diamond and Related Materials, **12** (2003) 1964.

[63] S. Asgary et al., Structure, morphology and electrical resistance of W_xN thin film synthesized by HFCVD method with various N_2 contents." Rare Metals, **39** (2020) 1440.